
Article:
Stone, D.A., Foster, M.P., Ballantyne, E.E.F. et al. (2020) A low cost, rapid impedance measurement technique suitable for Li-ion health diagnosis in battery energy storage systems. International Journal of Smart Grid and Clean Energy, 9 (2). pp. 346-356. ISSN: 2315-4462

https://doi.org/10.12720/sgce.9.2.346-356

International Journal of Smart Grid and Clean Energy

A Low Cost, Rapid Impedance Measurement Technique Suitable for Li-ion Health Diagnosis in Battery Energy Storage Systems

D. A. Stone [a]*, M. P. Foster [a], E. E. F. Ballantyne[b], H. Price[a]

[a] *Department of Electronic and Electrical Engineering, University of Sheffield, Sheffield, S1 3JD. UK*
[b] *Sheffield University Management School, University of Sheffield, Sheffield, S10 1FL. UK*

Abstract

Battery energy storage is becoming a vital part of green energy systems. Prediction of the state of health of energy storage systems is difficult as it relies on a number of parameters. Pseudo Random Binary Sequence (PRBS) excitation of energy storage batteries has been shown to be a valid method of battery parameter identification for lead acid batteries [1]. The purpose of this work is to validate PRBS test data from a 3Ah LiFePO4 cell forming part of an EV battery-pack cell against Electrochemical Impedance Spectroscopy (EIS) data obtained from an industry-standard potentiostat (Solartron 1480). PRBS results are obtained in under 200 seconds on easily reproducible equipment which can be built into a green energy battery management system, while the EIS process takes over two hours on prohibitively expensive laboratory equipment. This work validates PRBS as a fast and portable method of obtaining the impedance spectrum of Lithium Ion cells, which can then be used to obtain information about SoH of the BESS.

Keywords: Battery impedance measurement; Cell health prediction; BMS

1. Introduction

Lithium has the lowest density of any metal, and the highest electrochemical potential. With the advent of consumer portable electronics in the 1980's lithium batteries were developed for their excellent power to weight ratio, and pioneering work was commercialized by Sony in the early 1990's [2]. Lithium batteries are available with a large number of different electrode chemistries, but the main focus for secondary (rechargeable) batteries has been on Li-ion and Li-ion polymer batteries, until the 1990's mostly for the consumer electronics industry, but now also for large scale electric vehicle and grid Battery Energy Storage Systems (BESS) for renewable and green generation systems.

Lithium based battery technology is currently widely researched, and is also overlapping into development of both flow-battery [3] and metal-air battery [4] technology. Compared to older battery chemistries, Li-ion batteries have high specific energy (energy-to-weight ratio), are efficient, have long lifetimes, minimal memory effect and low self-discharge.

While Li-ion cells have high current capacity, this must be limited in practice to prevent internal heating and early failure. Safety has been a significant issue in bringing the consumer battery technology to market and Li-ion cells can only be safely operated in conjunction with a battery management system (BMS) providing at minimum over-voltage, under-voltage, over-current and over-temperature protection [5]. Larger utility scale systems will also require cell voltage balancing, as when cells are in series, the performance of the overall system can be limited by the performance of the weakest cell.

A Battery Management System (BMS) must perform three broad functions in order to maintain the safety of a Lithium based battery pack. These functions can be described in the context of a large array of

* Manuscript received May 4, 2019; revised January 7, 2020.
Corresponding author. *E-mail address*: d.a.stone@sheffield.ac.uk.
doi: 10.12720/sgce.9.2.346-356

Li-ion cells assembled into a battery pack, such as is found in a typical Energy Storage System (ESS) application.

1.1. Protect cells and battery packs from damage by keeping the battery within its Safe Operating Area (SOA)

Arguably the most important task for the BMS is to maintain a battery pack in a safe state. Battery packs consisting of parallel and series arrays of multiple cells can have very high energy density and the potential to deliver large fault currents, which could lead to catastrophic temperature rises and cascading failure of the cells. Manufacturers minimize this risk by creating sub-modules within larger battery packs, with features such as physical firewalls and fuses between modules, vents to control the direction of hot gasses and flames in the event of fire, and armor plating to protect against puncturing in vehicle applications [6].

In tandem to these physical safety measures, the BMS monitors pack electrical and thermal conditions to ensure that individual cells are kept within specification. Upper and lower voltage limits, maximum continuous charge/discharge currents and pulse currents are chemistry-specific and given in cell manufacturers datasheets alongside operational temperature ranges.

1.2. Maintain the battery to meet the requirements of its application

The operating conditions just described are those which must be adhered to in order to maintain safe functioning of the battery pack. Ensuring that these limits are enforced is a coarse function of the BMS, but its value extends beyond safety and the BMS may perform secondary and tertiary functions depending on the application. For instance the BMS in a laptop will alert the user when the State of Charge (SoC) reaches a critically low level. Once the SoC drops to a predefined level then the BMS might switch to energy saving mode, disabling inessential services before eventually taking control from the user and executing a safe shutdown sequence in order that the system be put into a safe state while there is still battery power to do so. Then the BMS isolates the battery from any new demands until it has been recharged to a predefined minimum SoC. In larger BESS, the BMS may disable the inverter operation to prevent further discharge if the battery SoC is too low, or overcharge if the battery SoC is too high.

1.3. Maintain the cells and battery packs to maximize the lifetime of the battery

A third function of the BMS is to prolong the useable life of the battery. Observing safety limits and application-specific functional limits may be considered the primary and secondary tasks for the BMS, while a useful tertiary task is to extend the life of the battery pack. There may be some overlap between the secondary and tertiary function of the BMS, and the mechanisms it uses to achieve these include battery equalisation, heating, cooling, parameter measurement, and controlling the distribution of load demand amongst the cells.

To ensure these functions are carried out, a number of useful battery metrics are available and may be inferred from simple measurements of cell / pack voltage, current and temperature. These metrics are commonly taken as: Battery State-of-Charge, (SoC) which is a measure of the remaining useful charge in a battery pack, usually given as a percentage of maximum possible charge. The charge capacity of a battery declines throughout its life-cycle therefore an accurate estimation of SoC requires that the present maximum charge capacity of the battery be known, as well as the amount of useable charge remaining. Therefore another metric is required to track these changes in charge capacity – and feed the calculation of SoC estimates – as it decreases from the nominal capacity of a new battery; Battery State-of-Health (SoH) is a parameter that reflects the present condition of an ageing battery in comparison with a new battery. As well as declining capacity, other parameters change over the lifetime of a battery. Internal resistance (or impedance) increases, maximum available power declines and the capability to support a given load is diminished. A third useful metric is State-of-Function (SoF) which is a measure of the battery's capability to perform a specific duty in support of the functionality of a system which is powered by the battery. SoF is a function of SoC, SoH and battery temperature.

In addition to the direct measurements of cell / battery voltage, current and temperature, cell / battery impedance measurements over a wide range of frequencies can provide a means of identifying the physiochemical processes in an electrochemical system. Electrochemical Impedance Spectroscopy (EIS) allows equivalent circuit parameters to be extracted which in turn may be correlated with physiochemical processes within cells.

As a battery is discharged, observed changes in the impedance spectrum can be used to identify SoC. Also, changes in impedance can be correlated to ageing effects within the battery and therefore feed SoH and SoF estimation algorithms within the BMS.

2. Battery Impedance Measurement

EIS is not normally carried out within a BMS system as EIS measurements tend to be carried out on single cells within laboratory conditions, utilizing expensive and highly accurate equipment. The main approaches to EIS measurement are:

2.1. Swept frequency sine measurements

The most common, standard approach to measuring impedance is to measure the system response to a small voltage or current stimulus of fixed frequency. The phase and amplitude of the response can easily be manipulated using fast Fourier transform (FFT) techniques to give the impedance as a function of frequency. An impedance spectrum of the system can be constructed by repeating the test over a range of frequencies; commercial instruments are available that sweep the frequency in the range of typically 1 mHz to 1 MHz, and directly produce an impedance spectrum in the form of a bode diagram or a Nyquist plot. The signal to noise ratio of this method is excellent – since frequencies of interest can be directly specified – however the measurement time required can be prohibitively long when low frequency data is needed [7]; low frequency response is an important aspect of the frequency response function (FRF) of an electrochemical cell [8].Ω

2.2. Transient measurements

Another method involves applying a voltage step-function V ($t<0$, $V=0$; $t>0$, $V=V0$) to the battery and measuring the resultant time-varying current, i(t). The quantity V0/i(t) is often called the indicial impedance, or time-varying resistance [9], and usually transformed into the frequency domain to show the frequency dependent impedance. The excitation in this case is non-periodical and therefore a suitable windowing function must be used to correct distortion in the impedance spectra. Another requirement is that V0 is kept sufficiently small that a linear system response is ensured.

2.3. White noise stimulation and broadband excitation

A signal composed of true white (random) noise will stimulate a system equally at all frequencies. Furthermore, this description can be relaxed to say that the requirement for a stimulus to be considered a white noise input to a system is that it has a flat power density spectrum over a frequency range much greater than the system bandwidth [10]. A stimulus of this type (i.e. one possessing a uniform power spectrum) will produce a system response that can readily be manipulated into providing the system frequency response using Fourier analysis.

There are three important advantages to this method of system identification over the two conventional methods described above [10]:

1. The system (battery) may be allowed to remain in its normal functioning mode, since the noise excitation is spread over a wide bandwidth and is necessarily of a low intensity so that the system is maintained operating within its linear region.
2. Measurements are not affected by other sources of noise, provided they are stochastically independent of the input noise source.
3. Stored energy in the system has no effect on the measurement of the impulse response.

However, there are two important disadvantages to this method. Accurate estimates of the cross-correlation function still require that the stimulus and response are measured for a long (ideally infinite) amount of time. Second, the stimulus energy must be kept small to ensure an approximately linear response is measured from a non-linear system. This increases the accuracy required in the measurement of the stimulus and response signals.

The measurement of the frequency response function (FRF) via broadband excitations has been demonstrated to take significantly less time than when using stepped sinusoidal excitation [11], given good signal-to-noise ratio (SNR) (this time advantage is reduced when the SNR is poor).

3. Approximation to White Noise

A pseudo-random noise source produces a frequency response that is similar to white noise except that it is produced deterministically and is therefore periodic, and the power spectral response is therefore only flat across a specific bandwidth; it is therefore considered to be a source of band-limited white noise.

A key reason for the early adoption and continued success of PRBS is that the signal can be generated easily with a minimum of digital hardware using simple shift register circuitry and appropriate feedback, Fig. 1. While several classes of pseudo-random binary sequences exist [12], maximum length sequences (MLS) are the class of PRBS signals that are generated in this way and will be referred to as 'PRBS' here.

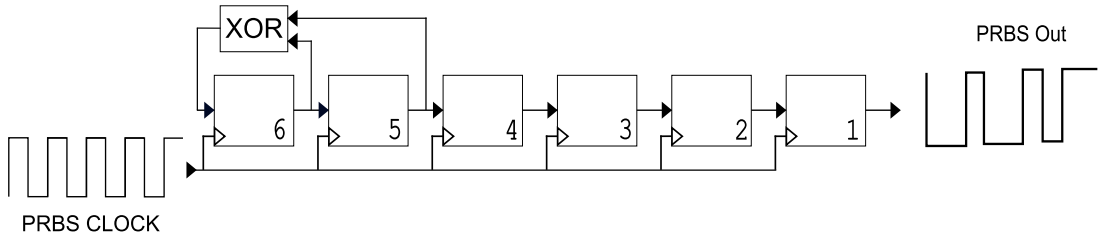

Fig. 1. 6-bit shift register showing the feedback tap connections used to produce a maximum-length sequence (MLS).

A shift register containing n storage elements will produce sequences of length. Thus the shift register shown in Fig. 1, will produce a PRBS such as that seen in Fig. 2.

The power spectral density (PSD) of this signal is shown in Fig. 3, where it has been normalized to show the power density as a function of generator clock frequency. The Fourier transform of a periodic signal is a line spectrum only having values at frequencies of

$$f = k / T \; Hz \tag{1}$$

'T' being the period of one complete sequence and 'k' an integer. These discrete values are given by (4) [10, 12], where 'V' is the amplitude and f_{CLK} is the shift register clock (the bit-rate of the PRBS stream).

Note that at the reciprocal of the clock pulse or its integer multiples, there is no power in the signal. It has also been shown [12] that as 'N' increases, the power in the first harmonic converges towards

$$\frac{2V^2}{N} \tag{2}$$

The slower decay of the spectrum as 'k' increases gives the desired flat response over the system bandwidth, the half-power point of which is approximately

$$0.443 \times f_{CLK} \tag{3}$$

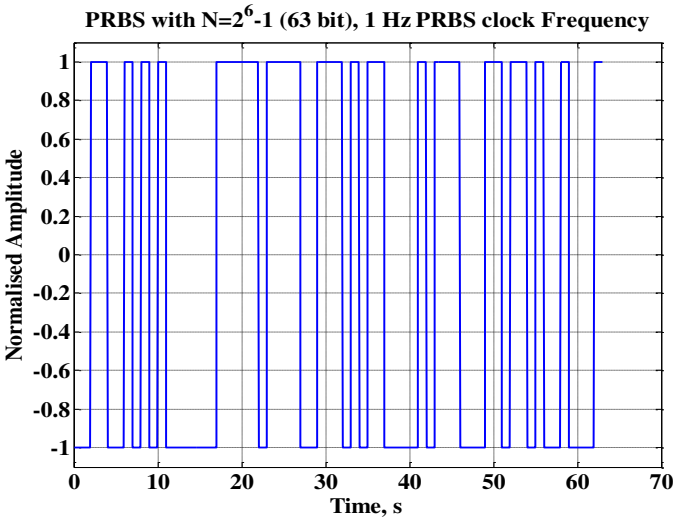

Fig. 2. A 1 Hz bipolar PRBS signal produced from a 6-bit shift register

In Fig. 3, this value is 0.429, as the PSD was produced by an N=63 (6-bit) PRBS shift register.

As stated previously, this method of system identification offers an advantage in the ability to stimulate many frequencies simultaneously with even power, reducing measurement time.

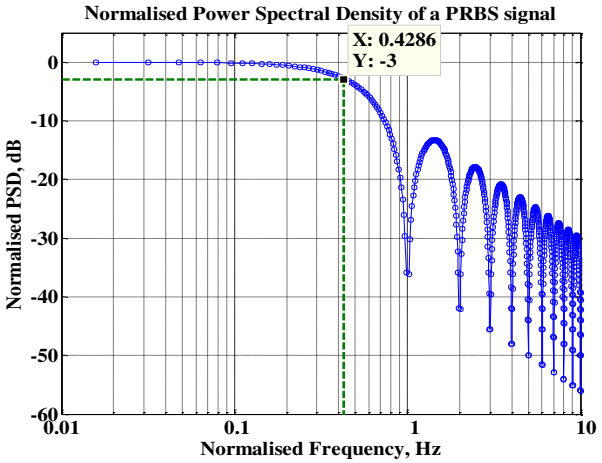

Fig. 3. Normalized PSD of the PRBS signal seen in Fig. 2

A large battery can more easily be kept within a linear region of operation throughout the identification process, and the impedance spectrum is easily obtained by dividing the power spectrum of the voltage response with that of the current stimulus (assuming a current controlled excitation).

$$S_{xx}(f) = \frac{V^2}{f_{CLK}} \frac{N+1}{N} \left(\frac{\sin(f\pi / f_{CLK})}{f\pi / f_{CLK}} \right)^2 \tag{4}$$

4. Test Set-up

For the purposes of this paper, the impedance measurement system runs in tandem with a high power battery cycler. When an impedance test is required, the battery under test is isolated from the charge

cycler using a Kilovac relay and control of the battery current transfers to the Arduino based PRBS control board, which is capable of drawing up to 2 A from the battery. The PRBS tests used were unipolar, only discharging the battery, therefore to minimize state changes while performing system identification tests, low stimulus currents were drawn from the battery during the PRBS testing. The test rig is shown in Fig. 4. The entire system is controlled and data logged using Labview.

The test method for measuring impedance at different SoC follows the format below (example values for 3 Ah LFP cells are used in parentheses):

1. The cells are discharged at a C/2 rate until the low voltage cut-off (2.6 V) is reached.
2. Cells are charged at a C/2 rate up to their maximum voltage cut off, and held there until the current reduces to a value of 3% of the C-rate (90 mA for a 3Ah cell).
3. The cells are again discharged at C/2 rate until they reach the low voltage cut-off (2.6 V for LFP cells).
4. Step 2 is repeated, and the cell is now considered to be at 100 % SoC.
5. The cell is taken offline for a set amount of time (at least 30 minutes). This is the relaxation (rest) time, which allows the terminal voltage to settle to a steady state.
6. An OCV reading is taken, the cell is then brought back online.
7. A PRBS impedance test is begun. This is broken into eight separate sequences of the same 63-bit MLS, at bit rates from 1 kHz to 1 Hz, which lasts 96 seconds. These are then repeated and it is the data from the second set which is then analyzed (as the cell terminal voltage has then settled from its initial 'on load' voltage drop into a steady load state) making the total impedance test time around 200 seconds.
8. The test then enters a repetitive cycle until the low voltage cut-off is reached:
   a. The cell is discharged by 10 % of its nominal capacity (300 mAh for a 3 Ah cell).
   b. Taken offline for a preset rest period (e.g. 30 minutes – same as step 5).
   c. PRBS impedance test is repeated.
9. Once the cell has reached 0% SoC (e.g. LFP cell terminal voltage reaches 2.6V) step 8a is terminated and steps 8b and 8c are allowed to execute a final time.
10. The cell is re-charged to 30% SoC (ideal storage state for Li-ion cells).

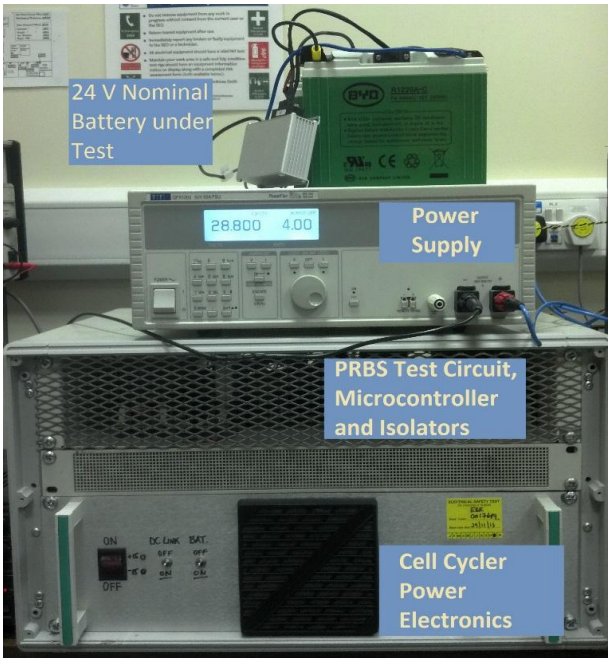

Fig. 4. Cycling rig and PRBS impedance tester

Table 1 shows the PRBS clock frequencies used and the resulting bandwidth of impedance measurable from each sample set in the sequence. The full test consists of two cycles of eight PRBS stimulus streams (16 total), and the post-processing is done on the final eight sequences – this allows the cell to recover from the initially severe voltage drop which results from being subjected to a load after being at rest. Differential measurement of terminal response voltage and stimulus current is done at 5 kS/s.

Table 1. Chosen PRBS Clock frequencies and resultant bandwidth of spectrum

Sequence #	PRBS Clock frequency	Useful frequency range after processing	Test duration for 63 bit PRBS (Single stream)
1 (9)	1 kHz	16 Hz – 330 Hz	63 ms
2 (10)	143 Hz	2.3 Hz – 47 Hz	440 ms
3 (11)	111 Hz	1.8Hz – 37 Hz	570 ms
4 (12)	55.6 Hz	0.9 Hz – 18 Hz	1.13 s
5 (13)	25 Hz	0.4 Hz – 8.3 Hz	2.52 s
6 (14)	12.8 Hz	0.25 Hz – 4.2 Hz	4.91 s
7 (15)	4 Hz	65mHz – 1.3 Hz	15.8 s
8 (16)	1 Hz	16 mHz – 330 mHz	63 s

Following a typical test such as that above, a single data file for each impedance test is generated. These contain the terminal voltage measured prior to the test, the SoC and temperature of the cell, and a data array consisting of [time, stimulus current, and response voltage]. The data array contains a continuous stream of all 16 sequences. A single set of 8 PRBS stimulus and response signals, is then processed to provide the impedance as below:

1. The 16 individual stimulus and response signals are extracted from the data array by cross-correlating the array with a clean reference signal for each PRBS clock frequency. The final set of eight sequences is used.
2. A DFT of the current and voltage, yields a signal power spectrum for each sequence.
3. The impedance spectrum (now in the frequency domain) is obtained from the voltage and current spectra.
4. The obtained spectrum is band limited to the useful frequency ranges listed in Table 1.
5. The eight spectrums are combined and averaged to yield the impedance spectrum for the battery under test

5. Results

The primary purpose of the work was to characterize various 3.2 V - 3 Ah 26650E LiFePO4 cells, although the intention was that the equipment be versatile enough to test other batteries and cells, such as 24 V - 20 Ah LFP battery packs and single 100 Ah – 3.7 V LTO polymer (pouch) SLPB cells. The test approach may also be embedded within BMS systems in larger BESS and be applied at a module level within the battery.

Presented here is a summary of the tests done on the 26650E LFP cells. Here, impedance vs SoC tests were carried out, along with basic SoH tests done by comparing the impedance spectrums of a new cell and an aged cell of known cycle life. The tests were carried out in a temperature controlled chamber, the temperature being held constant for the test duration. The temperature was varied between tests to achieve cell measurements in 10°C steps between 10°C and 50°C inclusive. Sufficient time was allowed after the change in chamber temperature to allow stabilization of the cell temperature before each test commenced.

5.1. 26650E LiFePO4 (LFP) cell capacities

These 3 Ah cells have a nominal voltage of 3.2 V. Table 2 lists the condition of the cells and the test configuration used (single or parallel), along with the reference numbers used in this section. Note that cell 1 was damaged during testing and was therefore only tested at 10°C, 20°C and 30°C. All other cells and configurations were tested up to 50°C.

Table 2. Cell reference table

Cell Reference #	Description
1	New cell, damaged during testing – incomplete data set (<30 cycles)
2	New cell, lightly cycled (<30 cycles)
3	New cell, lightly cycled (<30 cycles)
4	New cell (0 cycles)
5	End Of Life (EOL) cell (2300 cycles)
23	Cells 2 & 3 in parallel
234	Cells 2,3 & 4 in parallel

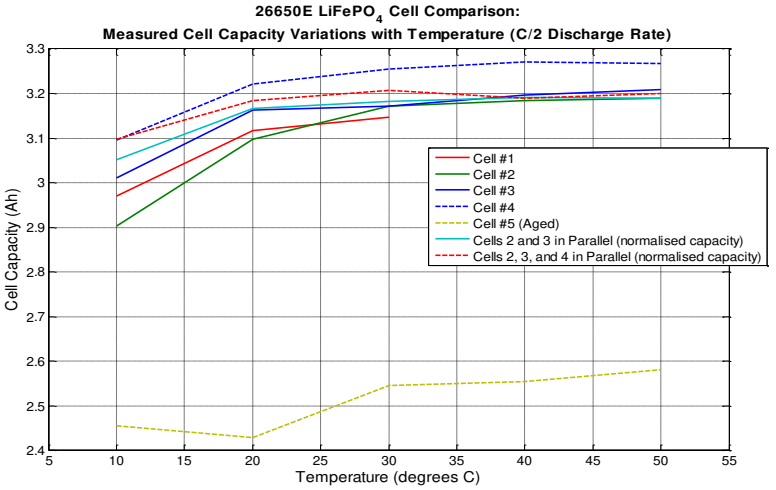

Fig. 5. Measured Cell Capacities

The measured cell capacities for the cells under test has been shown in Fig. 5. This illustrates the differences between the capacities of the new and aged cells. The aged cell having performed 2300 full charge / discharge cycles prior to the tests, but otherwise identical to the remaining cells. The cell parallel combinations have their capacities normalized to that of a single cell to allow direct comparison in Fig. 5.

Fig. 5 also shows the variation of measured capacity (Ah) with temperature. Cells 1, 2 and 3 show similar capacities, while cell #5 – which has been heavily cycled – has capacity reduced by approximately 15 % after 2300 cycles. Cell 4 was a new cell with zero cycles and shows the highest capacity. At low temperatures, a parallel configuration of cells allows more charge to be removed per cell (Normalized capacities shown). The overall trend for all the cells, and parallel combinations, is for an increase in useable capacity as the temperature is increased.

5.2. PRBS vs EIS impedance measurements

Having established the reduction in capacity of the aged cell, a comparison between the cell impedance measured with the proposed PRBS technique, and the impedance measured with a laboratory standard Solartron 1480 Electrochemical Impedance Spectroscopy (EIS) measurement system using a swept sine technique, allows the comparative accuracy of the proposed system to be assessed. The results of the two tests may be seen in Fig. 6, with both tests being carried out at 20°C (room temperature), held within the temperature controlled chamber.

The PRBS based impedance measurement is around 40 times faster (~200 seconds) than the measurement taken on the Solartron system and at a significantly reduced cost. A comparison of the results show good correlation apart from the results at 100 % SoC. This divergence of the results can be explained by different relaxation times prior to beginning the tests; the Solartron EIS test was initiated immediately after a full charge, with no voltage relaxation period preceding it in this case.

It can be seen in fig 6, that at frequencies above 0.5 Hz, both tests reveal little difference in impedance

as the SoC changes. However, the PRBS results diverge from the EIS measurements at frequencies above around 100 Hz, and this is thought to be due to the lack of synchronization between the PRBS generation clock and data acquisition clock. This gives rise to a small phase shift in the measurements which becomes more significant as the frequency of interest increases.

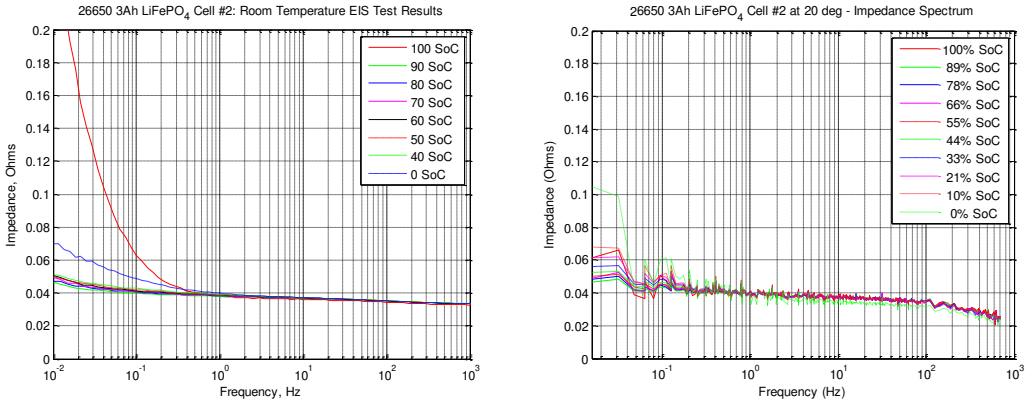

(a) (b)

Fig. 6. Comparison of EIS Swept Sine Results (a) with PRBS Impedance Results (b)

The comparison between the systems illustrates the possibility to obtain the cell impedance through fast application of PRBS techniques during cell cycling, with little loss of accuracy as long as a limited bandwidth for the tests is acceptable.

5.3. Effects of cell ageing on measurements

Here a comparison is made between an aged cell (2,300 cycles) and a new cell, with the aim of identifying characteristic changes by which SoH can be derived. One established indicator of SoH is the impedance of a cell, since this is known to increase over the lifetime of the cells (number of cycles). For this reason we look to the PRBS impedance data for a correlation between SoH and impedance, and to assess whether the measurements can be made in a relatively short timeframe in comparison to that required by a laboratory based EIS test system.

In Fig. 7, we see that the aged cell (#5, Table 2) has an higher overall impedance than the new cell, as expected, and the impedance tests on both show a similar variation of impedance with temperature at all temperatures in the test.

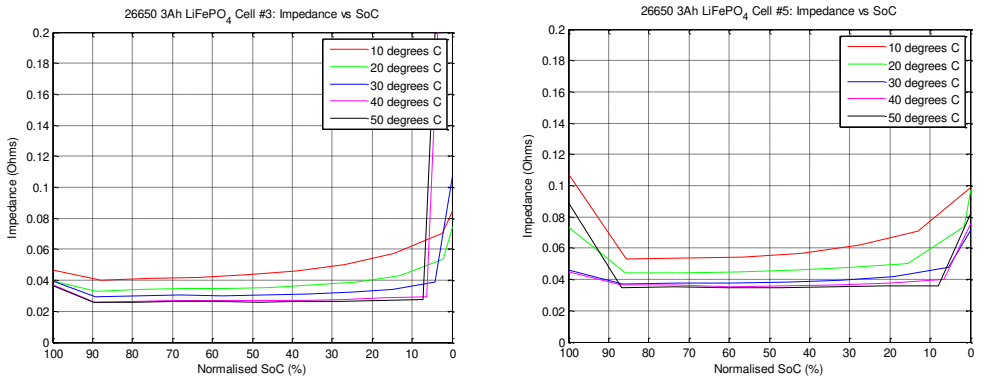

(a) (b)

Fig. 7. Comparison of New Cell (a) Aged Cell (b) Impedance Results, Measured using the PRBS Techniques

5.4. Comparison of impedance measurement techniques on passive components

Further validation of the accuracy of the impedance measurement technique may be found be the examination of a parallel circuit comprising of a 1Ω resistor in parallel with a 10mF capacitor. A Nyquist plot of the measured impedance is shown as Fig. 8.

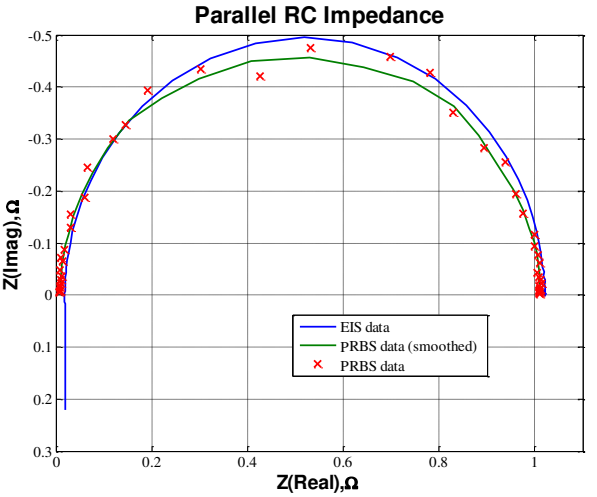

Fig. 8. Nyquist plot of parallel rc circuit validation test

Fig. 8 shows that the PRBS test has captured the characteristic semicircle of a parallel RC circuit. The low frequency points (right hand side) show good correlation with the EIS data (1.07 % error in real component, 0.17 % error in imaginary component), but these errors increase with frequency. Points on the Nyquist plot are not easily correlated to specific frequencies, therefore further analysis of errors is done on the amplitude and phase plots of Fig. 9.

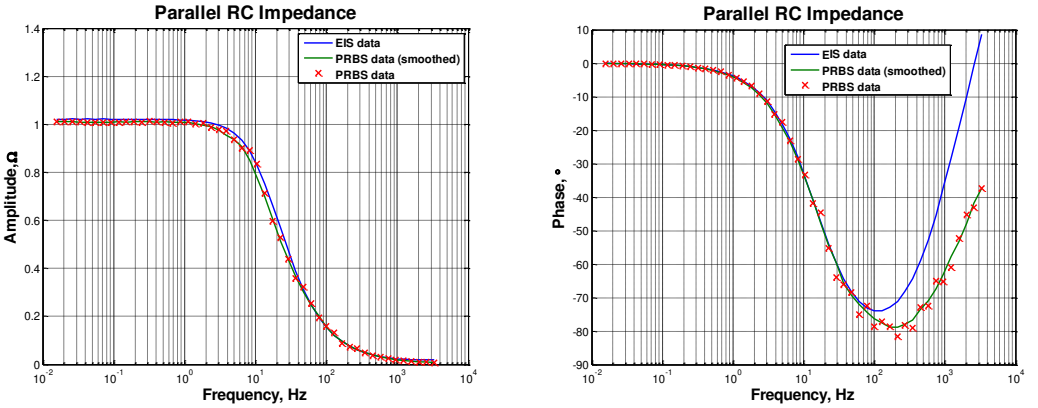

(a) (b)

Fig. 9. Parallel RC Impedance plots, R = 1 Ω, C = 10 mF

Fig. 9 shows that for frequencies below 100 Hz, there is good correlation between the standard data and the validation test data. The main difference is in the phase measurements at high frequencies, due to the non-synchronized sampling as discussed above.

6. Conclusions

This paper demonstrates a method of measuring cell / battery internal impedance, which is directly applicable to BESS, whether used in green energy systems or for vehicular applications. The accuracy of the technique has been demonstrated on both 'live' Lithium based cells, and on a passive electronic load, by comparison with laboratory standard electrical impedance spectroscopy (EIS) equipment. The technique has been demonstrated to run up to 200 times faster than the laboratory tests, and be able to be run on simple micro-controllers (Arduino for example), proving it is a suitable technique for inclusion into any green energy based BESS BMS systems.

Conflict of Interest

The authors declare no conflict of interest

Author Contributions

Prof. Stone supervised the work, wrote the paper and is the corresponding author. Prof. Foster supervised the work and proof read the paper. Dr Ballantyne co-wrote and corrected the paper. Mr Price carried out the work and produced the figures. All authors had approved the final version.

References

[1] Fairweather AJ, Foster MP, and Stone DA. 2011. Battery parameter identification with Pseudo Random Binary Sequence excitation (PRBS). *Journal of Power Sources*, 2011; 196(22): 9398–9406.

[2] Dunn B, Kamath H, and Tarascon JM. Electrical energy storage for the grid: A battery of choices. *Science*. 2011; 334: 928–935.

[3] Duduta M, Ho B, Wood VC, Limthongkul P, Brunini VE, Carter WC, and Chiang YM. Semi-solid lithium rechargeable flow battery. *Advanced Energy Materials*. 2011; 1: 511–516.

[4] Kraytsberg A. and Ein-Eli Y. Review on Li-air batteries: Opportunities, limitations and perspective. *Journal of Power Sources*, 2011; 196: 886–893.

[5] Vazquez S, Lukic SM, Galvan E, Franquelo LG. and Carrasco JM. Energy storage systems for transport and grid applications. *IEEE Transactions on Industrial Electronics*, 2010; 57: 3881–3895.

[6] Musk E. Tesla Adds Titanium Underbody Shield and Aluminium Deflector Plates to Model S. Tesla Motors, 2014.

[7] Sanchez B, Vandersteen G, Bragos R. and Schoukens J. Basics of broadband impedance spectroscopy measurements using periodic excitations. *Measurement Science and Technology*. 2012; 23: 105501.

[8] Jossen A. Fundamentals of battery dynamics. *Journal of Power Sources*. 2006; 154(2): 530–538.

[9] Barsoukov E. and Macdonald JR. eds. 2005. *Impedance Spectroscopy - Theory, Experiment and Applications*, Wiley.

[10] Davies WDT. Using the binary maximum length sequence for the identification of system dynamics. *Electrical Engineers, Proceedings of the Institution of*. 1967; 114: 1582–1584.

[11] Schoukens J, Pintelon RM. and Rolain YJ. Broadband versus stepped sine FRF measurements. *IEEE Transactions on Instrumentation and Measurement*. 2000; 49: 275–278.

[12] Godfrey K. Introduction to binary signals used in system identification. *International Conference on Control 1991*, 1991; 161–166.